Trends in Heat Stress over Europe

Bachelor Thesis

B. Sc. Physics of the Earth System:
Meteorology, Oceanography, Geophysics

Christian-Albrechts-Universität zu Kiel
GEOMAR Helmholtz Center for Ocean Research

Author: Nils Ole Niebaum

Matriculation Number: 1118884

First Examiner: Prof. Dr. Joakim Kjellsson

Second Examiner: Dr. Robin Pilch Kedzierski

December 2020

I. Abstract

During heat waves, heat stress becomes a serious health risk and can be lethal. Thus, heat waves are in line with the most dangerous natural threats for humans and the environment. We investigated how heat wave properties and occurrence changed over Europe during the period of 1900-2010 using the ECMWF twentieth century reanalysis data (ERA-20C; 1900–2010).

In this thesis, the heat wave definition of the German Weather Service (Deutscher Wetter Dienst - DWD) was chosen. To quantify heat stress, we used the unitless simple Wet Bulb Globe Temperature (sWBGT). The DWD heat wave definition was checked for multiple years during which strong and well-observed heat waves occurred.

We took a closer look at the climatology of the periods 1900-1930 and 1980-2010 and differences between both. Strong increases in the 98th percentile of the whole year daily maximum temperature and sWBGT were identified which exceeded the mean changes in general. The spatial patterns differed, especially over the Balkans.

Significant increases of mean heat wave days per year were identified over Europe with the greatest exceeding 6 heat wave days per year in a century over Italy, the Balkans and southern Turkey. The mean daily maximum sWBGT during heat waves increased by more than 1.5 per century over wide parts of central and eastern Europe. An increase of sWBGTX by more than 3 per century was found over France. It was shown that the distribution of daily maximum sWBGT during heat waves shifted by approximately 1 for the median and 0.8 for the 95th percentile over Europe allowing the upper 5% to pass harmful thresholds more often.

An increase of population exposure to harsh and to extreme heat stress over Europe was identified, by combining Gridded Population of the World, Version 4 (GPWv4) data set with ERA-20C. The strongest increase of the percentage of population exposed to high heat stress appeared over the Mediterranean region with significant trends of 25% per century for *harsh* and 15% per century for *extreme* conditions (defined in Section 3.4). The temporal evolution appeared to follow the Atlantic Multidecadal Oscillation phases, worth analysing in the future. After 1985 a strong increase in population exposure was identified in wide parts of Europe.

II. Zusammenfassung

Während des Auftretens von Hitzewellen kann Hitzestress zu einem ernsthaften Gesundheitsrisiko werden und ist u.U. sogar tödlich. Somit gehören Hitzewellen zu den gefährlichsten Naturkatastrophen für Mensch und Umwelt. Im Rahmen dieser Bachelorarbeit wurde untersucht, wie sich die Eigenschaften und das Auftreten von Hitzewellen über Europa im Zeitraum von 1900-2010 verändert haben. Dazu wurde die ECMWF-Reanalyse des zwanzigsten Jahrhunderts (ERA-20C; 1900-2010) verwendet.

In dieser Arbeit wurde die Hitzewellendefinition des Deutschen Wetterdienstes (DWD) zu Grunde gelegt. Eine Quantifizierung des Hitzestresses erfolgte über die einheitenlose "simple Wet Bulb Globe Temperature" (sWBGT). Die Hitzewellendefinition des DWD wurde für mehrere Jahre überprüft, in denen starke und gut beobachtete Hitzewellen auftraten.

In dieser Arbeit wurde die Klimatologie der Zeiträume 1900-1930 und 1980-2010 untersucht und die Unterschiede zwischen beiden genauer betrachtet. Dabei wurden starke Anstiege im 98. Perzentil der ganzjährigen täglichen Maximaltemperatur und in der sWBGT identifiziert, welche im Allgemeinen die mittleren Änderungen übertrafen. Die räumlichen Muster unterschieden sich insbesondere über dem Balkan.

Es konnte gezeigt werden, dass die mittleren Hitzewellentage pro Jahr über Europa signifikant zunahmen, wobei die größte Zunahme von mehr als 6 Hitzewellentagen pro Jahr innerhalb eines Jahrhunderts über Italien, dem Balkan und der südlichen Türkei zu verzeichnen war. Das mittlere Tagesmaximum der sWBGT (sWBGTX) während Hitzewellen nahm über weiten Teilen Mittel- und Osteuropas um mehr als 1,5 pro Jahrhundert zu. Eine Zunahme von sWBGTX um mehr als 3 pro Jahrhundert wurde über Frankreich festgestellt. Desweiteren hat sich die Wahrscheinlichkeits-Verteilung der sWBGTX für Hitzewellen über Europa verschoben. Eine Zunahme um etwa 1 für den Median und 0,8 für das 95. Perzentil wurden identifiziert, so dass die oberen 5% häufiger gesundheitsgefährdende Grenzwerte überschritten.

Durch die Kombination eines hochauflösenden Bevölkerungsdatensatzes (GPWv4) mit ERA-20C konnte gezeigt werden, dass in den Jahren nach 1985 in weiten Teilen Europas der Anteil der Bevölkerung, der extremem Hitzestress ausgesetzt war, zunahm. Der stärkste Anstieg des Anteils der Hitzestress-betroffenen Bevölkerung war über der Mittelmeerregion (MED) zu verzeichnen. Die zeitliche Entwicklung scheint dem Verlauf der Atlantischen Multidekadischen Oszillation zu folgen und ist ein interessanter Zusammenhang, der in folgende Studien untersucht werden kann.

III Table of Contents

1. Introduction

Heat waves are events of extraordinary high temperatures for an extended period and are in line with the most dangerous natural threats. During the years 1998-2017 over 166,000 human deaths were associated with heat waves [World Health Organization, 2020]. Nevertheless, those extreme weather events do not get that much attention as their impacts are not directly visible.

A uniform definition for a heat wave does not exist. The World Meteorological Organization (WMO) defined a heat wave in a very general way: *"A period of marked unusual hot weather (maximum, minimum and daily average temperature) over a region persisting at least three consecutive days during the warm period of the year based on local (station-based) climatological conditions, with thermal conditions recorded above given thresholds."* [World Meteorological Organization, 2018]. Because the WMO definition did not specify any temperature threshold, multiple definitions have been derived with a variety of thresholds and implementations to estimate unusual conditions. Many national Weather Services adapted these, depending on the regional climate conditions. For instance, the German Weather Service used a threshold of 28°C [Deutscher Wetter Dienst, 2020].

Human bodies generate metabolic heat which needs to be transferred to the surrounding to prevent hyperthermia. This is done by pure thermal conduction, thermal radiation and evaporative cooling, which is used when humans sweat. By the second law of thermodynamics, the surrounding temperature needs to be below the human body temperature, such that the first two mechanisms can occur. Even in conditions with high temperature, the evaporative cooling can be an efficient mechanism to prevent hyperthermia [Sherwood and Huber, 2010]. Heat waves can cause heat stress by hampering the natural cooling system of the human body, which can cause serious health issues. To measure heat stress the Wet Bulb Temperature (WBT) can be used. For a healthy person at rest, WBT exceeding 35°C for more than 6 hours may result in death due to hyperthermia. For a person in poor health or under strenuous work, even lower WBT values may be lethal.

A more accurate estimation of heat stress is the Wet Bulb Globe Temperature (WBGT) because it depends on all four meteorological variables on which sweating and heat stress depend: air temperature, humidity, wind, and solar radiation [Australian Bureau of Meteorology, 2020]. The WBGT can be estimated by the simplified Wet Bulb Globe Temperature (sWBGT), which depends only on temperature and humidity [Buzan et al., 2015]. Values of sWBGT exceeding 31.1 (unitless) were considered as *potentially dangerous* by the US Army and could lead to serious health problems [Sawka et al., 2003].

Throughout the last few decades, Europe has seen several heat waves with high temper-

ature anomalies, long duration and large spatial extents. In 2003 a strong heat wave centred over France caused approximately 40,000 deaths [Buzan et al., 2015]. The heat wave was caused by quasi-stationary anticyclones leading to anomalously low cloud cover, strong persistent solar radiation, low precipitation and dry soils [Black et al., 2004]. A heat wave centred over Russia in 2010 has been associated with around 55,000 deaths [Buzan et al., 2015] and was one of the strongest in the last century ranked by heat-stress related deaths. It had a duration of more than 49 days in wide parts of Russia, extraordinary temperature anomalies and wide spatial distribution [Barriopedro et al., 2011; Russo et al., 2015]. The heatwaves during 1972, 2003 and 2010 stood out as the strongest heat waves from 1950 until 2010 [Russo et al., 2015]. During the last 20 years, more than 130,000 heat stress related deaths for people older than 65 years were identified on global scales every year. These numbers increased to over 250,000 during 2019 [Watts et al., 2020].

As global warming was observed during the last century, it affected heat waves in the past and will influence them in the future due to the anthropogenic climate change [Masson-Delmotte et al., 2018]. Barriopedro et al. [2011] suggested that in the last 500 years (1500-2010) the running decadal frequency of extreme summers increased dramatically over Europe (see their Fig. 2). They have shown that temperature maximums above the 99th percentile have doubled in European regions in a single decade. The number of heat wave days has tripled from 1950 to 2018 and warming by 2.3°C was noticeable over Europe. The strongest increase in temperature is found over central Europe and a signal of anthropogenic climate change was identified [Lorenz et al., 2019]. The heat waves during 1950-2015 were ranked by Russo et al. [2015] based on their spatial extent and temperature anomaly. Most of the strong heat waves occurred over Europe between 2000 and 2015 [Russo et al., 2015]. The occurrence of high temperature extremes increased in a similar pattern around multiple regions of the world [Alexander, 2016; Russo et al., 2014].

Heat waves with high temperature anomalies and long duration, which bring severe heat stress, were projected to become more frequent by the end of the 21st century, both over Europe [Feyen et al., 2020] and globally [Dosio et al., 2018]. Hence, the rare and extreme heat waves of today may become more common during the 21st century [Masson-Delmotte et al., 2018]. A 1.5°C level of global warming will increase the population exposed to heat waves in the whole European Union [Feyen et al., 2020]. Strong levels of increase were identified over the Iberian Peninsula and the Baltics. A 3°C warming scenario would lead to 50-year extreme heat wave under current climate conditions occurring every 3 years in Southern Europe [Feyen et al., 2020]. Even though a strong increase was predicted, the

extreme heat wave over Russia during summer 2010 will still be a rare event under the climate scenarios RCP4.5 and RCP2.6 [Russo et al., 2014]. On global scales, a significant reduction of the prevailing increase of heat wave occurrence is possible if climate warming would be reduced from 2°C to 1.5°C [Dosio et al., 2018]. Warming of more than 7°C would lead to a strong increase of inhabitable zones, as the WBT would rise regularly above 35°C [Sherwood and Huber, 2010].

This thesis explores how heat stress has increased over Europe in the 20th-century. Methods and Data are described in Section 2, Results are shown in Section 3, followed by a Discussion in Section 4.

2. Data and Methods

2.1. Data

2.1.1. ERA-20C

This study used 2m air temperature and dew-point temperature from the ERA-20C reanalysis product [Poli et al., 2016], available at 1.125° horizontal resolution and in 6h timepoints (0:00, 6:00, 12:00 and, 18:00 UTC). Only data over land was used in this thesis, i.e. grid cells with more than 2/3 open ocean were masked out in this thesis. The ERA-20C reanalysis covers the period 1900-2010 and was produced, using the Integrated Forecast System (IFS) from the European Centre for Medium-Range Weather Forecasts (ECMWF) [Poli et al., 2016]. The product was computed in 24h cycles. A short forecast based on the prior conditions was performed for each cycle by a climate model with 30 minutes temporal resolution, T159 horizontal ($\sim$ 125 km) resolution and with 91 vertical levels up to 0.01 hPa. The forecast was then combined with the given observational data using an incremental four-dimensional variational (4D-Var) analysis to produce the best estimation as output values. The model was forced by observed sea surface temperature, sea-ice, and atmospheric composition assimilating surface pressure and marine winds. A strict quality control was performed and described in Poli et al. [2016].

The data performance around the world and Europe was analysed in Poli et al. [2016]. In general, the accuracy increased during the century as the number of surface pressure observations assimilated per month in ERA-20C increased from about 30,000 to 3.6 million. Climate indices are in line with multiple other reanalysis products. Nevertheless, it showed discrepancies if a rare coverage with observation data is available, both in temporal and spatial distribution.

ERA-20C had a lower accuracy during the early 20th-century over Europe due to fewer observations covering Europe, but climate indices are comparable to other products [Poli et al., 2016]. Since only surface pressure and marine wind observations were used for the 4D-Var analysis, the 2m air temperature and dew point temperature may have biases. A slight cold bias of 0.5-1 K in temperature throughout the 20th-century, with respect to nigh-time ship-based air temperatures observations, was identified by Poli et al. [2016].

2.1.2. GPWv4 Population Data

The Gridded Population of the World, Version 4 (GPWv4) by the Center for International Earth Science Information Network - CIESIN - ColumbiaUniversity [2017] is an accurate population density data set with 30 arc-second resolution. It was derived from roughly

13.5 million national and sub-national data sets. The 2020 population density data was retrieved at a 2.5 arc-minute resolution and re-binned onto the ERA-20C grid. The re-binning process is further discussed in Section 2.2.4.

2.2. Methods

2.2.1. Definition of Heat Waves

There is no universal definition for heat waves. This is mainly due to regional climate differences and regional cultural adaptations that lead to different impacts of events with similar temperatures and duration. The WMO defines a heat wave as a period of at least 3 days with unusually hot weather compared to the climatological conditions which occur in the warm period of the year [World Meteorological Organization, 2018].
The definition of a heat wave is crucial, as it affects the occurrence, regional differences and trends of heat waves [Robinson, 2001; Smith et al., 2013]. The influence of humidity and temperature vary depending on the used definition [Buzan et al., 2015]. Heat-wave definitions include either one or a combination of the two following conditions for near-surface temperature: exceeding a fixed threshold and a deviation from the climatology [Robinson, 2001].

In this thesis, heat waves are defined using the definition from the German Weather Services (DWD). It identifies a heat wave as a persistent period of at least 3 days with daily maximum temperature (TX) exceeding both 28°C and the 98th percentile of seasonal TX based on a reference period from 1961 to 1990. For each day of the year (d) the 98th percentile was calculated from a distribution of TX for ±15 days around the investigated day (d) for 1961-1990. The distribution, A_d, may be written as the union,

$$\mathrm{A_d} = \bigcup_{y=1961}^{1990} \bigcup_{i=d-15}^{d+15} \mathrm{TX}_{y,i}.$$

Thus, TX must be seasonally exceptional and exceed 28°C for at least 3 days in a row to be considered a heat wave [Deutscher Wetter Dienst, 2020]. The fixed threshold of TX = 28°C was chosen to reflect very warm conditions in Germany and parts of Central Europe, but such a definition would miss most heat waves in Northern Europe [McCarthy et al., 2019; Russo et al., 2015]. As an example, the Swedish Weather Services defined a heat wave as a period of 5 consecutive days with TX exceeding 25°C, allowing heat wave events for unusual hot Swedish summer days [Swedish Meteorological and Hydrological Institute, 2011].

Other approaches were used in the literature. Robinson [2001] defined heat waves using a fixed threshold for day and night values of a Heat Index (HI) and used the 99th percentile as a threshold. The usage of hot days and tropical nights to identify heat stress increase performed by Fischer and Schär [2010] is similar. Furthermore, Fischer and Schär [2010] identified heat waves based on a similar percentile threshold and a duration of at least 6 days. Thus, they neglected short heat waves (3 to 5 days duration).
Heat waves can also be defined using only seasonally exceptional temperatures with no fixed threshold [Feyen et al., 2020; Russo et al., 2014, 2015], i.e. unusually warm conditions rather than absolutely warm *and* unusually warm conditions compared to the DWD definition. A more detailed overview of the heat wave definitions which were mentioned above can be found in Table A1.

The DWD definition was chosen, as it depends on TX values rather than on heat stress indices. There were multiple commonly used heat stress indices whose estimation quality of heat stress depends strongly on the weather conditions (sunny, cloudy, windy etc.) and the human behaviour as well as physical conditions (healthy, age, working or at rest etc.). Thus, temperature is preferable as it is a fundamental thermodynamic variable in meteorology and was readily available as 2m air temperature in the ERA-20C data-set. TX is a common value used in multiple heat wave definitions.

Daily maximum 2m temperatures were extracted for each day in the ERA-20C 6-hourly data set and were used as TX in this thesis, which most certainly is an underestimation of the real daily maximum temperature of the reanalysis product because in general, this occurs in between 12:00 and 18:00 UTC. sWBGT values were calculated for each time point based on Equation (2) using 2m temperatures and dew point temperatures from the ERA-20C data-set. The daily maximum sWBGT (sWBGTX) values were then chosen independently of TX.

2.2.2. Definition of Heat Stress

Multiple indices for heat stress were introduced and compared by Buzan et al. [2015], who separated those indices into three main types: indices that quantify comfort, indices that quantify the physical response, and empirical indices derived from thermo-physiology models to quantify the relation between weather condition and e.g. labour efficiency. An example of the last type is an index to quantify how much work may be done per time and weather situation.

Even in conditions with high temperature sweating can be an efficient cooling mechanism

for humans, but its efficiency depends not only on the surrounding temperature, but also on humidity, wind, and solar radiation. Decreasing efficiency of sweating results in heat stress and can lead to serious health issues and hypothermia with lethal consequences [Sherwood and Huber, 2010]. The WBGT is an empirical index and is well suited for quantifying heat stress because WBGT was designed for precisely this purpose, further it is based on all four meteorological variables on which heat stress depends: temperature, humidity, wind, and solar radiation.

In this thesis, the sWBGT was used as the heat stress indicator [Australian Bureau of Meteorology, 2020] which is derived from temperature and humidity, but not from wind and radiation as WBGT is. The sWBGT assumes a person to be exposed to moderate sunshine and light wind. Overestimation of thermal stress can occur especially in cloudy and windy conditions and when the sun is low.

To calculate the unitless sWBGT, equation (7) from Buzan et al. [2015] was used:

$$\mathrm{sWBGT}(T, \mathrm{RH}, e_{\mathrm{RH}}) = 0.56 \cdot T + 0.393 \cdot \frac{\mathrm{RH}}{100} \cdot e_{\mathrm{RH}} + 3.94, \tag{1}$$

with the vapor pressure e_{RH} in mbar corresponding to the relative humidity RH in % and temperature T in °C.
Using the equation (25) from Sonntag [1990], the saturation water vapour pressure $e(T)$ of temperature T in °C is:

$$e(T) = 6.1094 \cdot \exp \frac{17.625 \cdot T}{T + 243.04}.$$

The dew point temperature (T_{dp}) could be used to modify Equation (1).
With $\mathrm{RH} = \frac{e(T_{dp})}{e(T)} \cdot 100$ and $e_{\mathrm{RH}} = e(T_{dp})$ it can be said that $\frac{\mathrm{RH}}{100} \cdot e_{\mathrm{RH}} = e(T_{dp})$ and the Equation (1) could be rewritten as :

$$\mathrm{sWBGT}(T, T_{dp}) = 0.56 \cdot T + 0.393 \cdot e(T_{dp}) + 3.94. \tag{2}$$

Heat stress impact on humans can be divided into sWBGT threat levels (Table 1), which correspond to the proposal by Buzan et al. [2015] and Sawka et al. [2003].

Table 1: sWBGT threat levels suggested by Buzan et al. [2015] and Sawka et al. [2003]

alert	caution	potential danger	dangerous
$26.7 \leq \mathrm{sWBGT} \leq 29.3$	$29.4 \leq \mathrm{sWBGT} \leq 31.0$	$31.1 \leq \mathrm{sWBGT} \leq 32.1$	$32.2 \leq \mathrm{sWBGT}$

A shaded place indoors already reduces the heat stress and would lead to an overestimation of sWBGT [Australian Bureau of Meteorology, 2020]. Moreover, the proportion of people affected by heat waves depends on regional and cultural adaptations and the demography of the population [Watts et al., 2020]. These quantifications were not performed in this theses, as they would have exceeded the scope of this study.

2.2.3. Definition of European Sub-Regions

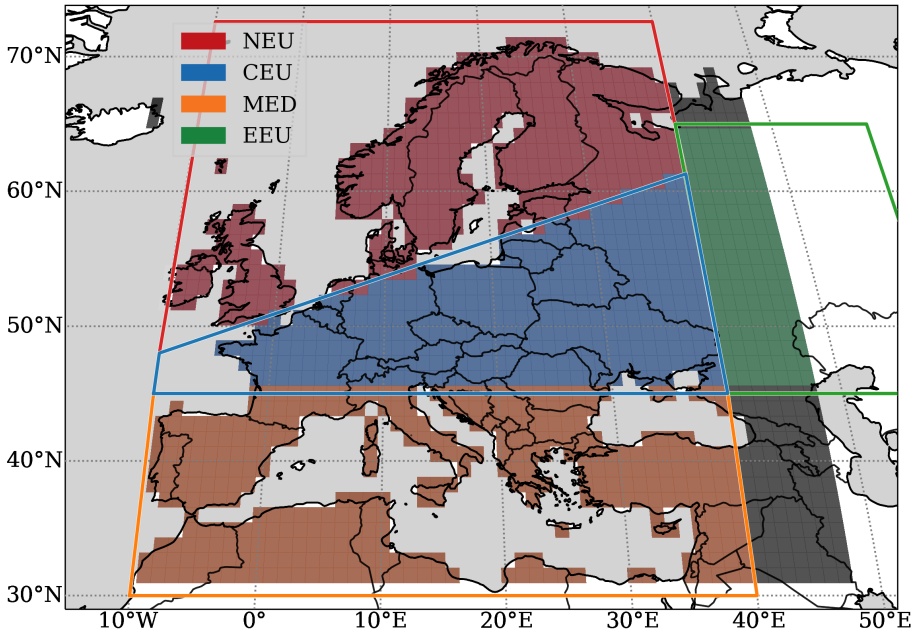

Figure 1: Spatial extent of the sub-regions used in this study. In red Northern Europe (NEU), in blue Central Europe (CEU) in Orange Mediterranean Europe and Africa (MED) and in green the Eastern Europe (EEU). Colored contour lines as region boundaries defined by Iturbide et al. [2020].

Four European sub-regions used in this thesis were based on the definition by Iturbide et al. [2020]. Because of their relatively different climate, these regions were used to analyse regional differences. Northern Europe (NEU) consists of Britain and Ireland, Scandinavia and parts of Northern Germany and the Netherlands. Central Europe (CEU) includes the central European countries North of 40°N latitude. Eastern Europe (EEU) is found East of Moscow and is the smallest region. The Mediterranean region (MED) includes all nations along the Mediterranean coast including North Africa. These regions are shown in Figure 1

2.2.4. Combination of GPWv4 and ERA-20C Data

To analyse how heat stress affected the European population, GPWv4 population data was re-binned to the ERA-20C grid for a combined analysis.

First, the population data was converted from population density, σ_{pop}, to total population, T_P, using the area A of each GPWv4 grid cell,

$$A_P = L^2 \cdot \Delta\Phi_P \cdot \Delta\lambda_P \cdot \cos(|\Phi_P|),$$

where λ_P, Φ_P are longitude and latitude on the GPWv4 grid and $\Delta\lambda_P \Delta\Phi_P$ are the horizontal resolutions, all in degrees. The distance $L = 111.32km$ is equal to 1° latitude. Total population of each grid cell is thus $T_P(\lambda, \phi) = \sigma_{pop} \cdot A$. The total population of the GPWv4 dataset is 1127 millions people in the Euro-Mediterranean region (Figure 2a).

The GPWv4 data was re-binned to the ERA-20C grid by summing up the population of the GPWv4 grid cells intersecting each ERA-20C grid cell, based on the simplified geographical distance (D) between GPWv4 and ERA-20C grid-points. D between two points was calculated using:

$$D = R \cdot \sqrt{(\Delta\Phi)^2 + (\cos(\Phi_m) \cdot \Delta\lambda)^2},$$

with the Earth radius $R = 6371.009km$, as well as $\Delta\lambda$ and $\Delta\Phi$ as the zonal and meridional difference between both points and Φ_m as the mean latitude of both points, all in radians, and using .

The re-binning-process can place some populations over the sea which would be masked out in our analysis. The total land population of the re-binned data set is 1049 million people which is 78 million less than in the original GPWv4 data. Thus, population re-binned out over sea were added to the population of the closest land point within a 100 km range. This led to a corrected total population of the re-binned data of 1121 million people, which is within 0.5% of the original GPWv4 population data. The total population of GPWv4 and the corrected re-binned product using ERA-20C grid can be seen in Figure 2.

2.2.5. Climatology and Trends

The climatology values of variables and their mean and upper percentile were derived for the first 31 years (1900-1930; including 1930) and the last 31 years (1980-2010) of the available data. The difference between those two spatial distributions was used to identify

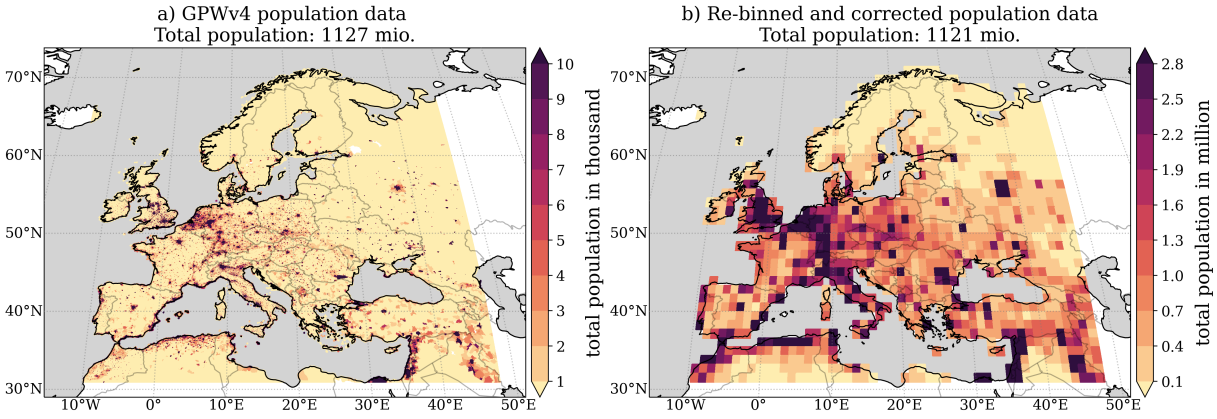

Figure 2: Total population of a) GPWv4, b) re-binned and corrected onto the ERA-20C grid.

climate changes. Furthermore, temporal trends were calculated for the whole time series (1900-2010). Those trends then were used to compare temporal evolution to the literature and gave a clear statistical signal of long-term changes. To enable confidence of 95% for the linear regressions used in this thesis, p-value $\leq 5\%$ were chosen as significant. The two-sided p-value used in this thesis indicated the probability that the null hypothesis is confirmed by *Chance*, whereby the null hypothesis was that the slope of the linear regression was zero.

3. Results

3.1. Climatology State and Changes

3.1.1. Mean Climatology and Changes of TX and sWBGTX

Overall TX was found to decrease with latitude (Figure 3a,b), although there was also a clear difference between continental and marine climates, where eastern Europe was colder than western Europe. The mean TX exceeded 21°C in most of the Mediterranean area for the time period 1900-1930 and 1980-2010. The mean TX did not exceed 17°C in most regions of CEU and was below 11°C in the Western parts of Russia during the first period. The TX was roughly 17°C across the Black Sea, which suggested that heat waves would have occurred here as often as in the central and Western CEU.

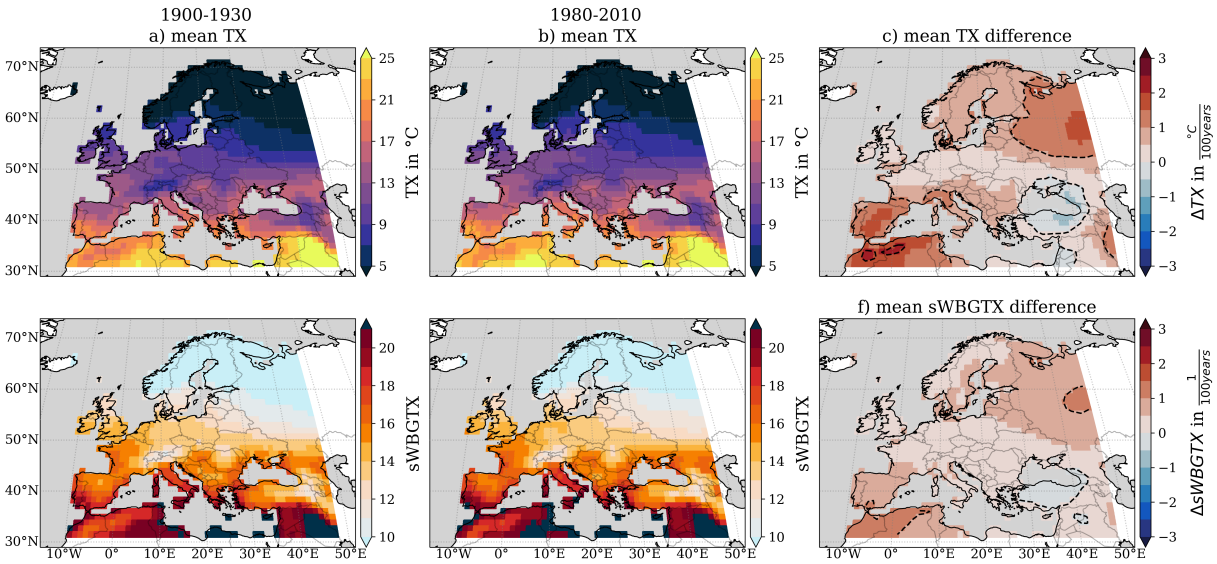

Figure 3: whole year mean TX and sWBGTX during 1900-1930 (a,d) and during 1980-2010 (b,e). (c,f) difference between the two periods. Differences (ΔTX and ΔsWBGTX) were standardised from 80 years to 100 years by multiplying with 100/80. Dashed lines as number differences.

Despite the general patterns been the same for both periods, the differences between them indicated regional diversity. All regions experienced an increase in the climatology TX except the regions bordering the Eastern Black Sea. The increase in TX was strongest over Russia and the Iberian Peninsula rising to 1.5°C per century, whereas the increase was lower than 0.5°C per century over central Europe and the British Isles. This is roughly half of the global mean temperature increase of approximately 1°C during the 20th-century [Masson-Delmotte et al., 2018].

The climatology of sWBGTX whole year mean (Figure 3d-f) followed a similar pattern

as the climatology of TX with an overall southwest-to-northeast gradient. The mean sWBGTX reached 15 along most of the Mediterranean regions and exceeded 20 across Southern Italy, Southern Greece, South West of Spain, the Israeli and North African coast. The changes in sWBGTX were in line with the spatial pattern of TX changes but with lower magnitudes.

3.1.2. Extreme Values Climatology and Changes of TX and sWBGTX

The whole year 98th percentile of TX (TX98) exhibited a similar gradient over Europe as TX (Figure 4a,b). TX98 values exceeded 32°C along most Mediterranean coastlines and exceeded 34°C over the Balkans, Southern Russia, and around the Black Sea, whereas 38°C appeared over parts of Northern Africa. TX98 between 24 and 26 °C occurred over France, Germany and Poland.

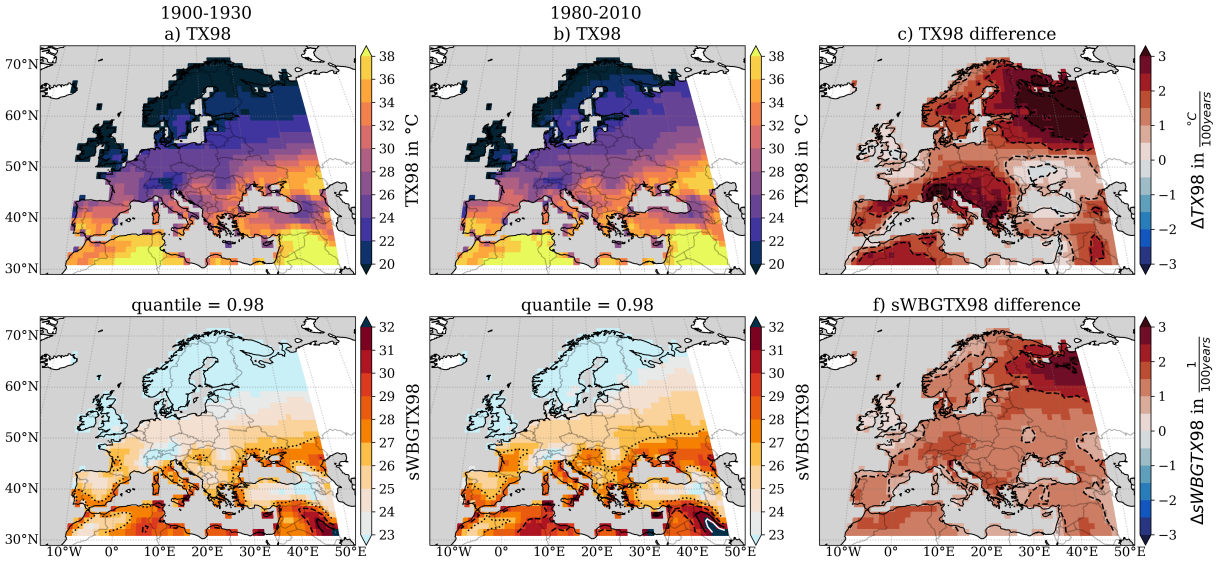

Figure 4: whole year mean TX98 and sWBGTX98 during 1900-1930 (a,d) and during 1980-2010 (b,e). (c,f) difference between the two periods. Differences ($\Delta TX98$ and ΔsWBGTX98) were standardised from 80 years to 100 years by multiplying with 100/80. Dashed lines as number differences. (b,e) Contour lines as sWBGT threat levels (Table 1): alert (dotted black), caution (dashed black), potential danger (solid black), dangerous (solid white) (see Table 1).

The differences in TX98 between 1900-1930 and 1980-2010 exceeded 1°C per century in wide areas of Europe (Fig. 4c), i.e. more than than the increase in TX (Figure 3c), which implies that the distribution of TX not only shifts towards higher values but also widens. However, the patterns of increase in TX and TX98 showed some discrepancies. The strong increase over Northern Russia moved further North and West compared to Figure 3. The changes of TX98 exceeded 2.5°C per 100 years in wide areas of Northern Russia and Finland and even changes of over 3°C were seen in the North East of Finland

and Russia. Furthermore, strong increases in TX98 of 2.5°C per century were located along the Adriatic sea, which reached across Northern and central Italy towards the Balkans and Greece. An increase in TX98 of over 2°C per century was observed over the Iberian Peninsula, Morocco and Algeria, while less than 1°C per 100 years increases were identified in the North of France and the UK and North, further TX98 slightly decreased South of the Black Sea.

The sWBGTX98 reached 27 during both periods across Italy, the Greek Islands, the East coast of Spain and around Southern Ukraine and Russia. The sWBGTX98 exceeded 29 along the Northern Tunisian, Egypt, the coast of Israel, Syrian and Cyprus. These values were associated with the threat level *alert* and might have led to health problems (Table 1; [Buzan et al., 2015]). An excess of 25 during the first 30 years and 26 during the last 30 years Across was found over CEU.

The increase in sWBGTX98 was overall larger than those of sWBGTX in general and exceeded 1 per century across the whole European region, except the UK, Ireland, and Northern France with increases of less than 0.5 per century (Fig. 4f). As for TX, this indicates that the distribution of sWBGTX shifts towards larger values and also widens. The sWBGTX decrease over northern Turkey was not seen for sWBGTX98. Moreover, the increase across the Balkans and Italy showed weaker magnitude compared to Northern Russian increase, where differences exceeded 2 per century, even though TX98 differences were similar for both regions. Thus, the differences of sWBGT98 were influenced by humidity more than those of sWBGTX between both periods.

3.2. Heat Waves of 1972, 2003, and 2010

To test the used heat wave definition, the summer heat waves of 1972, 2003, 2010 were investigated, because they were standing out as the strongest heat waves from 1950 until 2010.

The 1972 heat wave was centred over Western Russia and Ukraine (Figure 5a-c) with more than 10 heat wave days over a large area and up to 20 heat wave days East of Moscow. This could have been either be a single long-lasting heat wave or multiple heat waves appearing during summer 1972. In comparison to the reanalysis by Russo et al. [2015], a shift of the main area was seen from Scandinavia towards Russia and the Black Sea (Figure 5c). The shift appeared, because the TX threshold of 28°C was not used by Russo et al. [2015] and it suppressed heat waves across Finland compared to their results.

sWBGTX reached 26 in the mean during the 2003 and 2010 heat wave events over West-

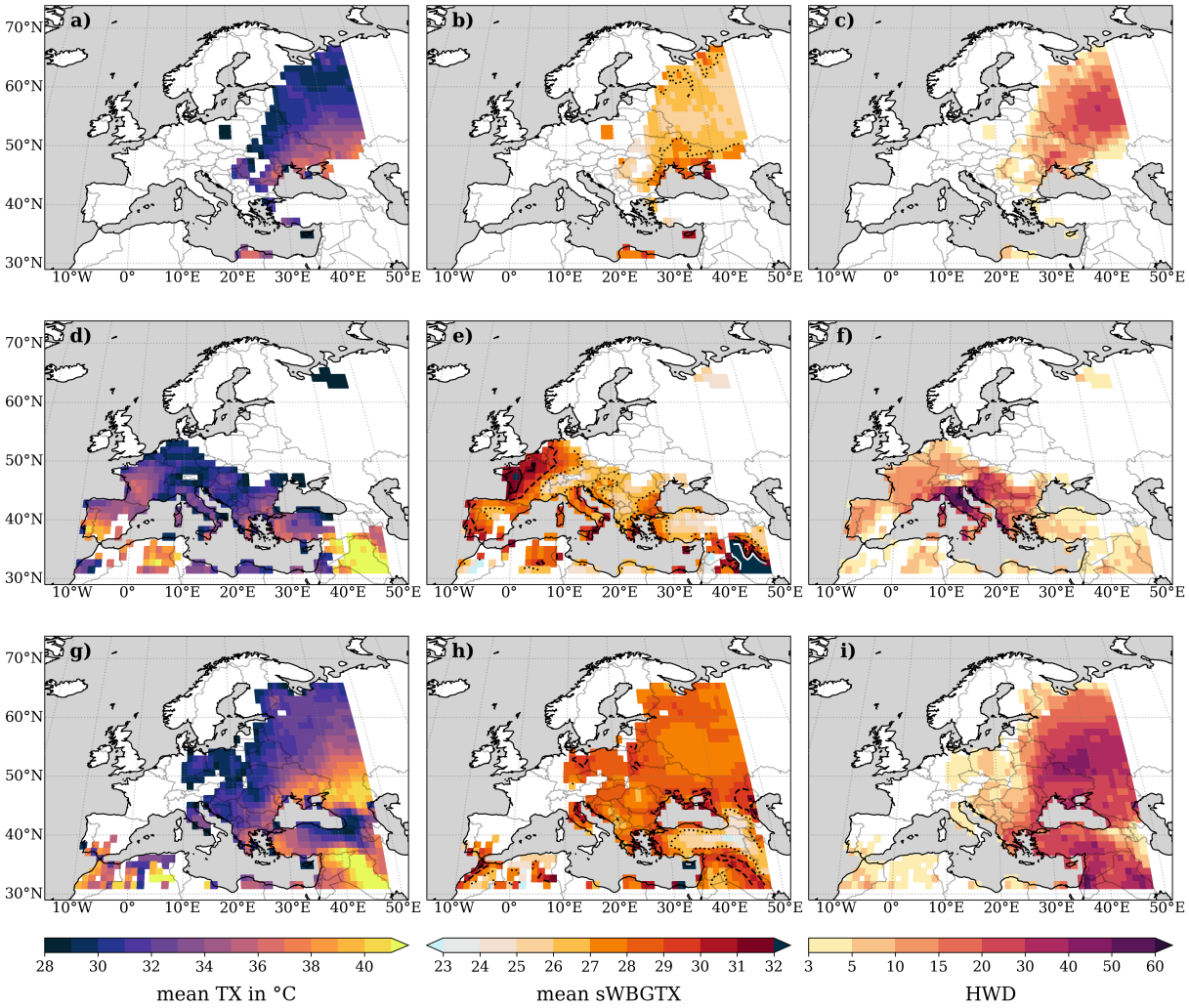

Figure 5: Mean TX (a,d,g), mean sWBGTX (b,e,h) and heat wave days (c,f,i) for all heat waves in 1972 (a-c), 2003 (d-f), 2010 (g-i). Heat wave examples were chosen based on their ranking in [Russo et al., 2015]. (b,e,h) Contour lines as sWBGT threat levels (Table 1): alert (dotted black), caution (dashed black), potential danger (solid black), dangerous (solid white) (see Table 1).

ern Europe during 2003 (Figure 5e), which was a level of alert (Table 1) and therefore strongly affected the population. It exceeded the climatology mean sWBGTX by more than 12. The highest values of sWBGTX were observed in coastal regions along the Crimea, with values rising above 29. The TX was a few degrees above the threshold of 28 °C along Northern Russia which is why the threshold restricted heat wave occurrence over Scandinavia and led to the spatial distribution difference regarding other papers e.g. Russo et al. [2015] and Barriopedro et al. [2011].

A very different regional pattern was seen for the heat wave in summer 2003 (Figure 5d-f). The regions with most heat wave days were found across Northern Italy, where more than 50 heat wave days occurred. More than 30 heat wave days were identified across Italy

and Croatia. A long duration was also observed across the North-Western Balkans and the coast of the Adriatic Sea with more than 20 heat wave days. More than 10 heat wave days were identified across France, the Western parts of Germany and Spain. The spatial distribution found in this thesis was slightly different compared to the investigations by Russo et al. [2015], who found the main region to be the North of France including Paris. Nevertheless, the spatial expansion found here was in line with the outgoing long-wave radiation anomalies demonstrated by Black et al. [2004], which indicated high temperatures in similar regions as seen in Figure 5. The mean sWBGTX pattern was much more similar to the results by Russo et al. [2014] and Barriopedro et al. [2011] (see Supporting Online Material Figure S7). The regions with sWBGTX greater than 29 appeared in the North of France, Belgium, the Netherlands and Western parts of Germany. Even values above 31 were observed in Northwest France. Those values exceeded potential dangerous conditions and might have led to serious health risks (Table 1; [Buzan et al., 2015]). High sWBGTX exceeding 32 led to serious health risks across Syria and Northern Iraq, but those areas are not discussed in this thesis.

During the 2010 heat wave, more than 20 heat wave days appeared in a large area, which spread from Israel, the Anatolian Peninsula and Greece, along the Black Sea up to the North of Russia (Figure 5h-j). The spatial pattern reached further South and West compared to Russo et al. [2015] and Barriopedro et al. [2011]. But the extraordinary extent of more than 40 days in large parts of Eastern Europe was in line with both analyses. The sWBGTX exceeded 27 in wide regions, except the higher and drier Anatolian plateau further values greater than 28 appeared in areas with less than 10 heat wave days, for instance, Eastern Germany, Northern Balkans and Italy.

3.3. Heat Wave Properties

Because years without heat wave occurrence implicated 0 heat wave days per year, the mean heat wave days per year (HWD/yr) was able to inferior 3 (Figure 6e,f), which were fewer days than the minimum duration of a heat wave.
During the period of 1900-1930, the highest value of over 3 HWD/yr appeared over Ukraine and Southern Russia (Figure 6e). More than 2 HWD/yr emerged over Turkey, Syria and Israel. Regions with more than 1 HWD/yr occurred across parts of the Balkans and Italy. Wide parts of CEU, MED and EEU were exposed to at least 1 HWD/yr in the mean. Regions without heat wave appearance were the North and Southeast of Germany, the Alps, the UK and Scandinavia.

In general, much more HWD/yr were identified across the whole European area during the

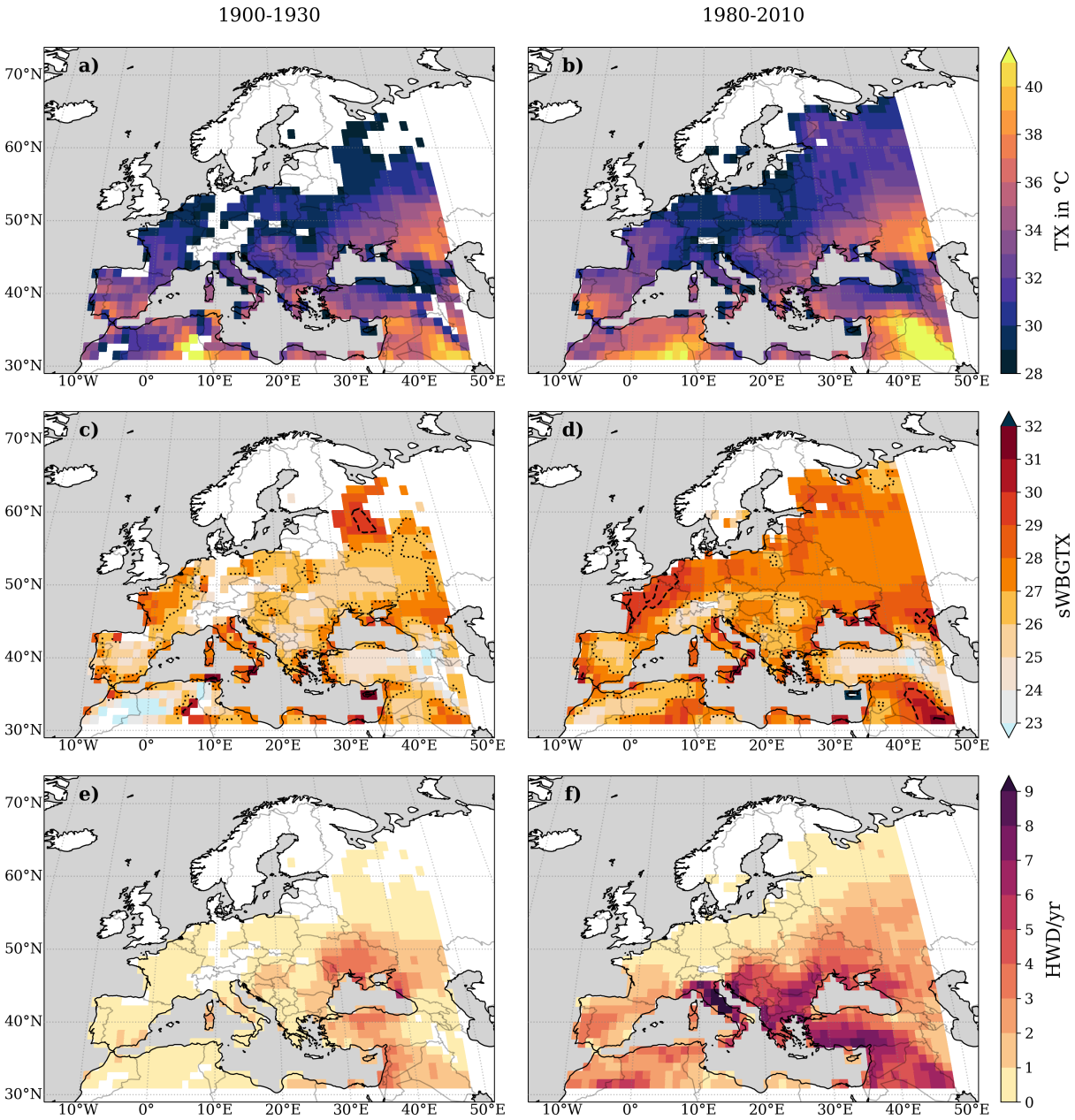

Figure 6: Mean TX (a,b) and sWBGTX (c,d) for heat wave days. (e,f) mean heat wave days per year (HWD/yr). All three for the periods 1900-1930 (a,c,e) and 1980-2010 (b,d,f). (c,d) Contour lines as sWBGT threat levels (Table 1): alert (dotted black), caution (dashed black), potential danger (solid black), dangerous (solid white) (see Table 1).

period 1980-2010 (Figure 5f), whereby Italy, the Balkans and the South coast of Turkey stood out being exposed to more than 7 HWD/yr on average. Areas affected by more than 3 HWD/yr had been rare during 1900-1930 but were observed over wide regions of MED and Eastern CEU during the latter period of 1980-2010. The whole CEU area experienced at least a single heat wave during this period, except Western Austria.

An increase in heat wave occurrence was identified over wide areas of Europe (Figure 7e,f).

The highest increase exceeded 8 HWD/yr/century and occurred over Italy and countries bordering the Adriatic Sea which is equal to an increase of more than 500% over Italy. The Balkans and Southern Turkey experienced an increase of 6 HWD/yr/century, equal to an increase of at least 300%. An increase of more than 3 HWD/yr/century was identified over the Iberian Peninsula and North of the Balkans. No significant trends appeared over wide regions of CEU but the differences between both periods indicated a rise of HWD/yr.

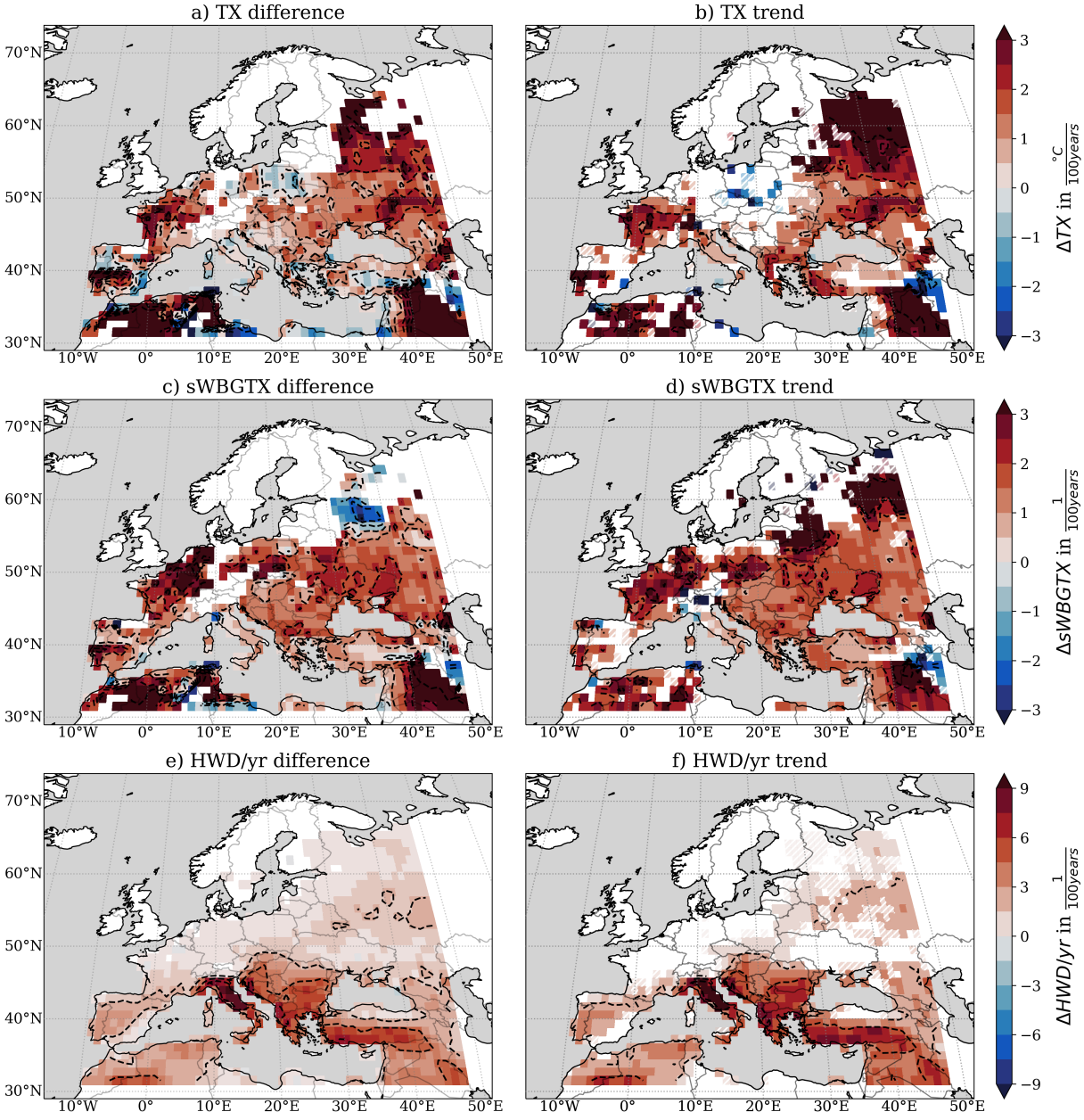

Figure 7: TX (a,b), sWBGT (c,d) and heat wave days per year (HWD/yr) (e,f). Differences between 1900-1930 and 1980-2010 (a,c,e). Significant trends for the period 1900-2010 ($p \leq 5\%$) (b,d,f). Hatched areas were non-significant trends with $5\% \leq p \leq 10\%$. (a-f) standardised to 100 years. Dashed lines indicated whole numbers (a-d) and multiples of three (e,f).

These trends and differences of heat wave days per year showed a similarity to the increase of temperature extremes (TX98 in Figure 4c). Those revealed a much stronger increase across the Balkans and Italy than TX (Figure 3c). Nevertheless, the strong increase in TX98 across the Northern parts of Russia and Scandinavia did not lead to a strong increase in the heat wave occurrence, comparing both periods. Most certainly, the threshold of 28°C was still not reached there.

The spatial distribution of TX had gradients as seen for those of HWD/yr (Figure 6e,f). A different pattern appeared compared to TX98 mean values. The significant trends of TX differed from TX98 changes. An increase of over 3°C per century was identified in Northern Russia as observed for TX98 change. But the strong increase over the countries bordering the Adriatic Sea was not visible in TX during heat waves. Values did not exceed 1°C per century there. The mean TX during a heat wave did not change much, but the occurrence and/or the duration of those events increased (Figure 7). Furthermore, an increase of more than 2°C per century was seen in trends and differences over the North West of France.

The pattern of mean sWBGTX differed from TX, due to the different changes in humidity. During the 1900-1930 period, sWBGTX means had been above 25 and exceeded 27 for 1980-2010 across Europe, except the Alps and the Anatolian plateau (Figure 6b,c). Both periods showed similar patterns in sWBGTX, but sWBGTX exceeded 29 across Northern France, Germany and the Baltic countries only in the later period. High sWBGT values were observed over the North West of France and especially along the Mediterranean and the Black Sea coasts where values exceeded 29. Values greater than 30 were identified along the Adriatic and the Black Sea coastlines and Cyprus. The Iberian Peninsula and the Balkans were exposed to more heat wave days, but based on their semi-arid climate, sWBGTX did not exceed 26, which was lower than over the West CEU.

sWBGTX was less correlated to TX during heat waves than it was the case for the whole year mean and 98th percentile.

sWBGTX increased by more than 1 per 100 years over the CEU region and trends larger than 2 per century appeared in the Western and North Eastern CEU. Differences and trends exceeded 1 per century across the Balkans and were lower over Italy. An increase of more than 0.5 was visible North of the Black Sea. High regional differences were identified over the Iberian Peninsula. In general, the spatial pattern of HWD/yr and sWBGTX changes and trends seemed to be not correlated. The temporal evolution of sWBGTX over Eastern Europe seemed to be based on humidity increase because TX did not increase over those areas. On the other hand, the sWBGTX increase was in line with

the TX rise over France.

To further understand how heat stress during heat waves evolved, the probability densities of sWBGTX during heat waves were derived for the periods 1900-1930 and 1980-2010, which were normally distributed for all regions except the NEU (Figure 8). The distributions of TX were not normal (not shown here), which supports the hypothesis, that TX and sWBGTX were not well correlated. Due to the normal character of the sWBGTX distributions, it could be concluded, that the heat stress was normally distributed in spatial and/or temporal manner. In other words, each grid point had a narrow normal or not normal distribution of heat stress and/or each grid point had a normal distribution of heat stress. To understand how the normal distribution occurred, further investigations would have been necessary.

Shifts of the sWBGTX medians were identified as 1.4 for CEU, 1.2 for EEU, 0.8 for MED, and 1 for all areas combined (Europe), but this should be considered carefully, as the distributions were not perfectly normal. The upper 5% of sWBGTX exceeded the potentially dangerous threat levels in the EEU rarely and never in CEU during 1900-1930, but exceeded those threat levels more frequently during 1980-2010 (Figure 8d,f). The 95th percentile shifted by approximately 1 for CEU and 0.6 for EEU. A narrowing of the distribution was observed for MED (Figure 8h). The 95th percentile increased by 0.8 for MED, which was less than the shifts over EEU and CEU. Nevertheless, the upper 5% were higher for both periods and exceeded the potentially dangerous conditions frequently during the 1980-2010 period.

It was evident, that higher heat stress during heat waves appeared more frequently over Europe in general and the upper 5% reached severe heat stress more regularly over Europe, due to a increased the 95th percentile by 0.8 (Figure 8i,j). The upper 5% of sWBGTX increased slightly less compared to the median. This was different to the non-heat wave related sWBGTX98 and sWBGTX differences between both time periods, which indicated much stronger increases for the extreme values (Figure 3f and Figure 4f).

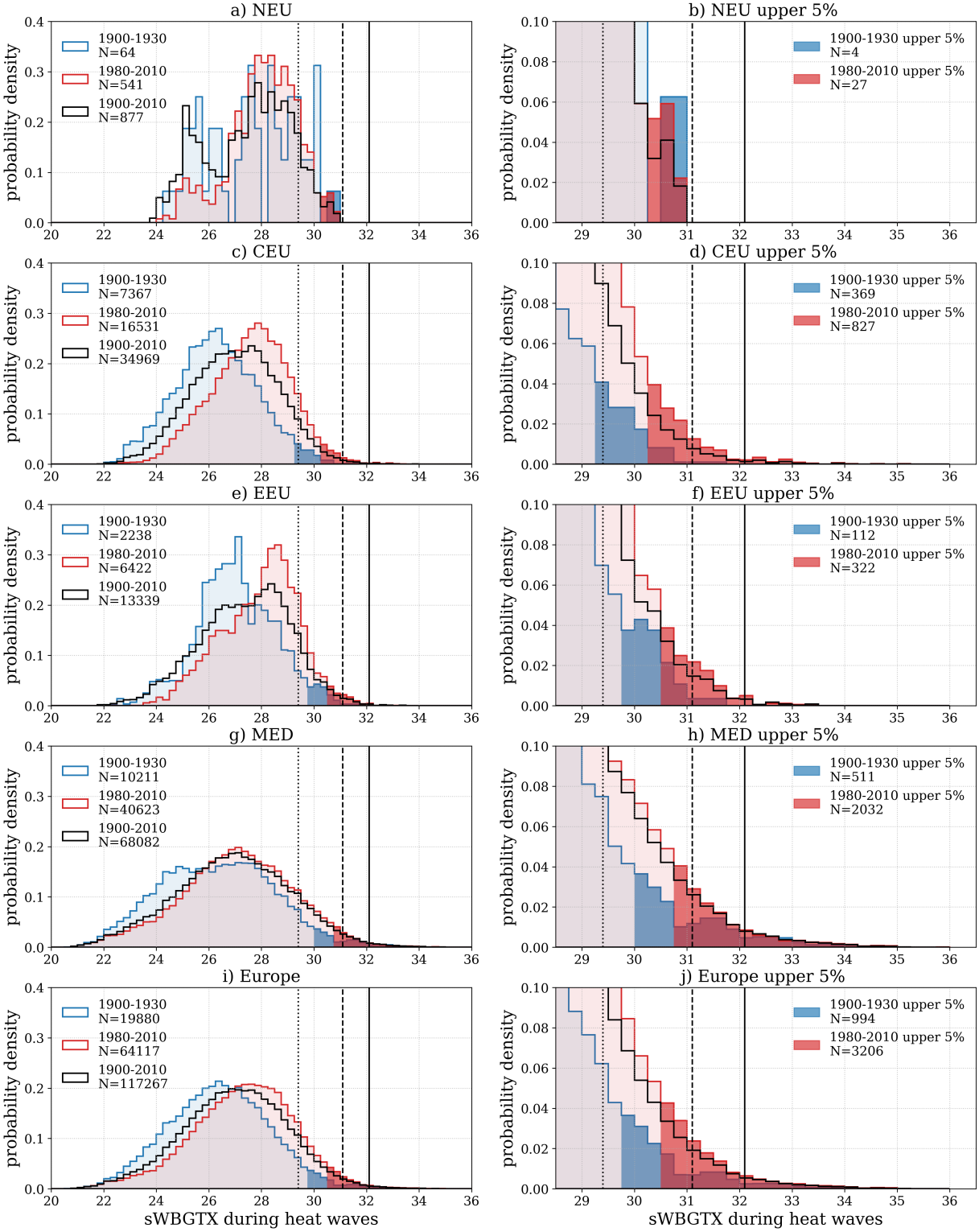

Figure 8: Probability density of sWBGTX during heat waves (a-j). Blue colour 1900-1930 period, red colour 1980-2010 period and black 1900-2010 period. Intense filled bins are part of the upper 5%. The vertical black lines indicate sWBGTX threat levels: caution (dotted), potential danger (hatched) and dangerous (solid) (Table 1; [Buzan et al., 2015]). Sum of all heat wave days for all grid points in the region during the period: N.

3.4. Exposed Population

The spatial pattern of European population exposed to at least 3 HWD/yr for which sWBGTX needed to exceed its 98th percentile from 1900-2010 (Figure 9a,b) was similar to the HWD/yr magnitude distribution (Figure 6e,f) for both time periods. The Heat stress was regionally extraordinary during these events because sWBGTX exceeded the whole year mean sWBGTX by more than 10 (Figure 3 and Figure A3) and the conditions most certainly led to a strong impact on the. The above conditions were described as *harsh* in the following (e.g., harsh conditions, harsh heat stress).

During the first 30 years, wide areas of Ukraine, Southern Russia and the Anatolian Peninsula were largely affected by harsh conditions for at least for 5 years (which we identified as regular). Hatched areas fulfilled harsh conditions for at least 2 years, covering the Balkans, around the Black Sea and North France.

During the period of 1980-2010, the spatial pattern of the regularly exposed population to harsh conditions was much greater and included nearly the whole MED and large parts of CEU and EEU. The Northern parts of Italy, Budapest and Moscow were high populated regions and experienced those conditions regularly during 1900-1930 but during 1980-2010 much wider parts of the European population were exposed to those conditions regularly. The German population experienced at least 2 years with regionally harsh heat stress during 1980-2010, which had not occurred during 1900-1930.

The temporal evolution of the exposed population indicated that most people were exposed in MED and the CEU (Figure 9c). The number of the total population exposed to harsh conditions exceeded 100 million for most years during 1910-1965 and remained below 100 million until 1985, whereafter the numbers increased. During the years 1998-2010 in general at least 300 million people were affected by harsh heat stress in the MED and CEU area.

The temporal evolution of the exposed population was analysed with the percentage of population exposed in each region (Figure 9d). A Gaussian smoothing with $\sigma = 2$ years was used for the solid lines. An increase in the exposed population appeared from 1910 onward with a decrease after 1950 for MED and CEU. The percentile of the population exposed in MED ranged between 10 % and 20 % during the period of 1920-1955. A period of less than 10 % exposure for both regions lasted until 1980, whereby the increase around 1972 was caused by the 1972 heat wave (Figure 5a-c). After 1980 the exposed population to harsh conditions increased intensely and exceeded 25% in CEU, and 40 % in MED after 1998. Even though years with harsh heat stress exposure occurred earlier (1943, 1945) but the frequency after 1990 was much higher compared to the 20th-century. The EEU

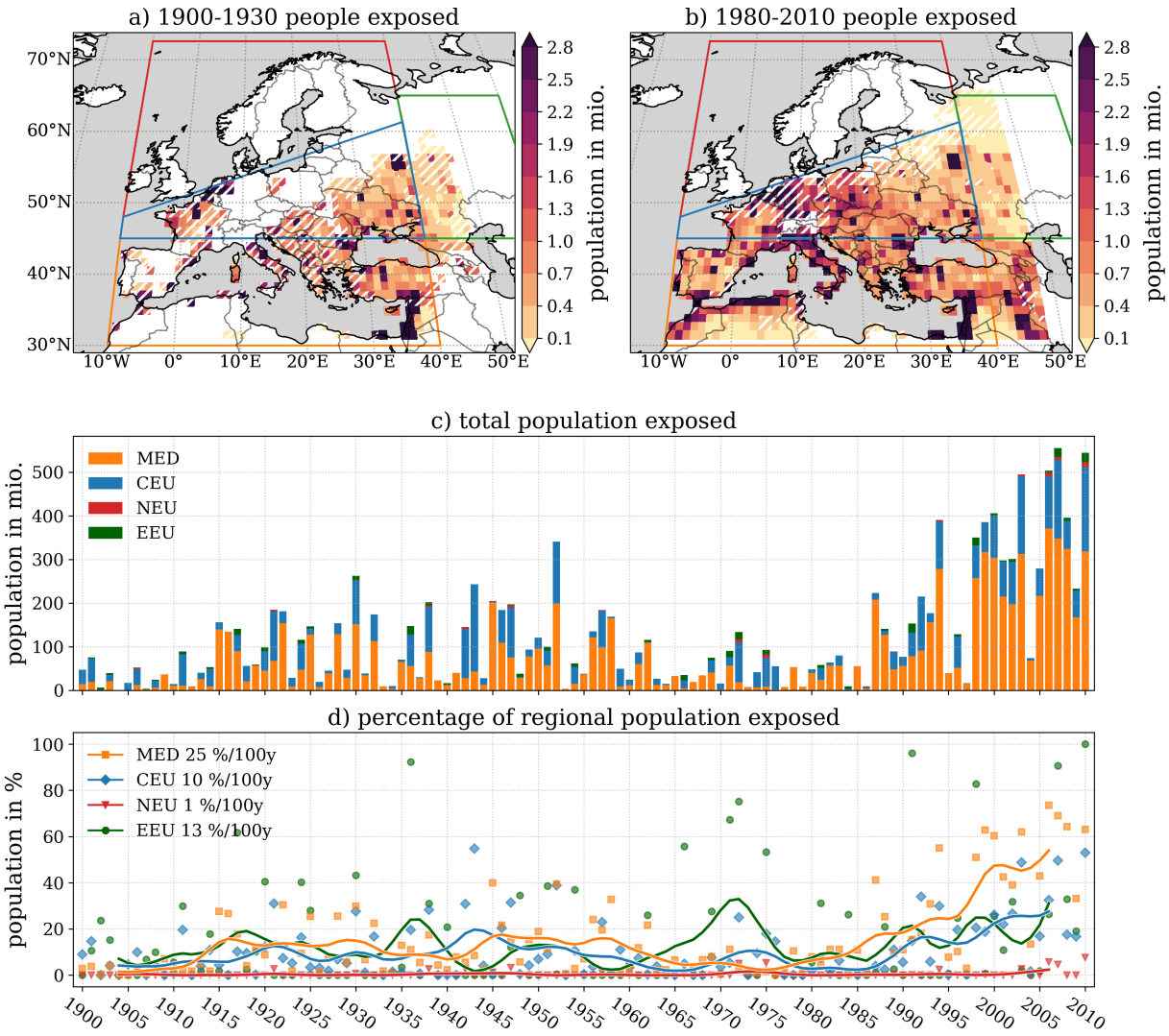

Figure 9: a) 1900-1930 and b) 1980-2010 with population exposed to at least 3 heat wave days per year with sWBGTX $\geq$ 98th percentile (1900-2010). (a,b) Areas met conditions for at least 2 years are hatched and solid if for at least 5 years. The colour represents the total population corresponding to the grid point. c) Total population exposed for each region. d) Percentage of the regional population affected, solid lines indicate Gaussian smoothing ($\sigma = 2$years). Significant trends for each region in the legend.

did not show a temporal evolution similar to those of CEU or MED and experienced 13 years with more than 40 % of its population exposed to harsh heat stress throughout the time series.

The strongest significant trend of the percentage of the exposed population was identified for MED with an increase of 25%/century. Increases of 10% per century for CEU and 11%/century for EEU were observed. On the other hand, a trend of 1%/century appeared for NEU, which was much lower compared to the other regions.
Similar trends were observed for population independent data (Figure A1), whereby MED

population-based trend exceeded the population independent trend by 6% per century.

The threshold of at least 3 HWD/yr for harsh conditions was increased to 6 HWD/yr to compare trends with stricter thresholds. Thus, at least 6 heat wave days per year needed sWBGTX values above the 98th percentile and were described as *extreme* (e.g., extreme conditions, extreme heat stress) (Figure 10).

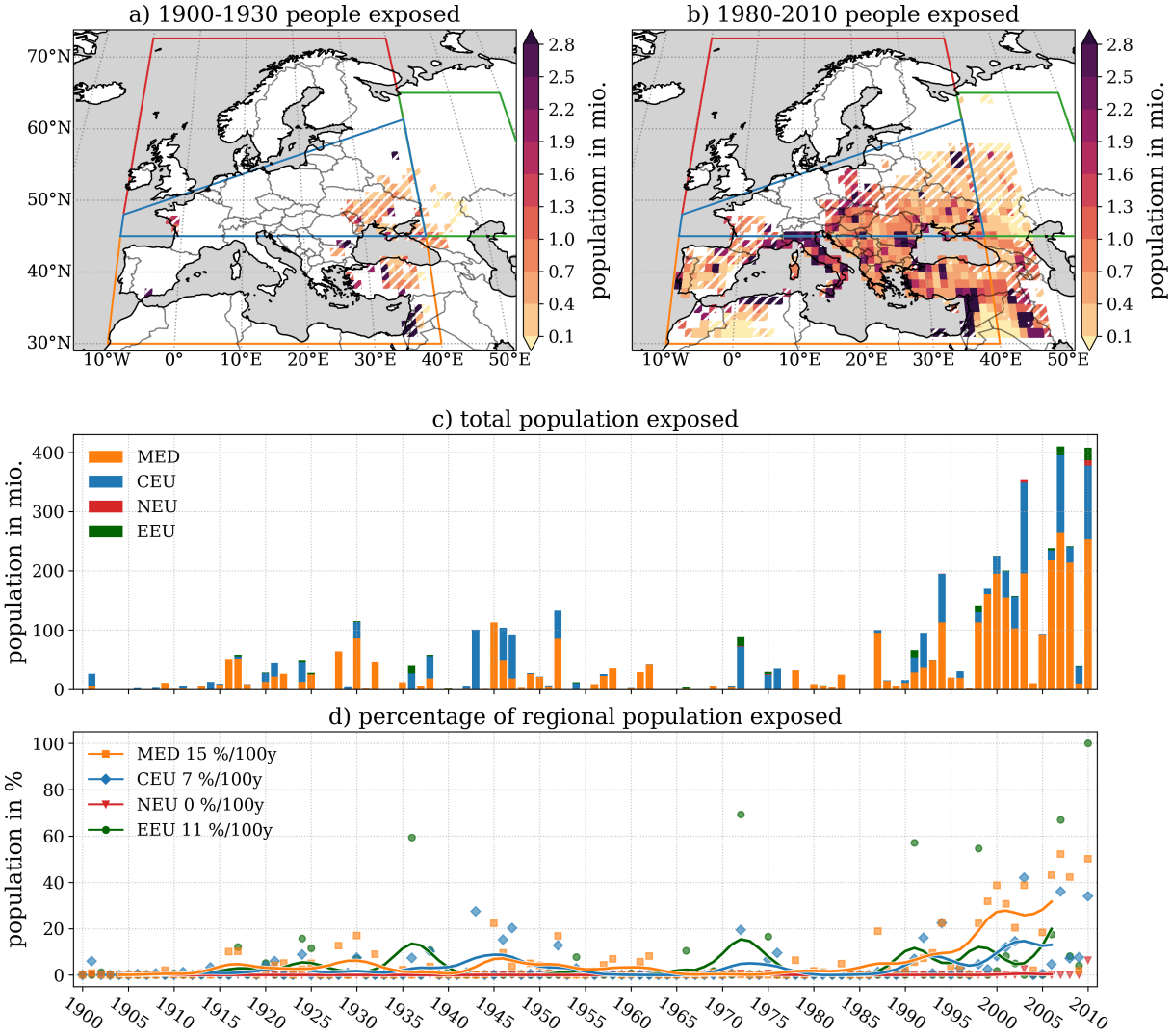

Figure 10: a) 1900-1930 and b) 1980-2010 with population exposed to at least 6 heat wave days per year with sWBGTX $\geq$ 98th percentile (1900-2010). (a,b) Areas met conditions at least 2 years are hatched and solid if for at least 5 years. The colour represents the total population corresponding to the grid point. c) Total population exposed per region year. d) Percentage of the regional population affected, solid lines indicate Gaussian smoothing ($\sigma = 2$years). Significant trends for each region in the legend.

The population affected by extreme conditions was less compared to harsh conditions shown in Figure 9. During 1900-1930, no region was exposed for more than 5 years to extreme heat stress (Figure 10a) but exposure for at least 2 years was identified North

and South of the Black Sea, in the West of France and Israel (Figure 10b). This pattern changed drastically from 1900-1930 to 1980-2010. During 1980-2010, a regular exposure (at least 5 years) to extreme heat stress was identified over Italy, the Balkans, Bulgaria and Turkey, whereby these regions include the high populated Northern Italy and the Danube Delta which experienced less or no extreme heat stress during 1900-1930. The pattern for extreme conditions during 1980-2010 was similar to that of harsh heat stress (Figure 9a,b). This pattern was more in line with the trends in HWD/yr than with trends of sWBGTX during heat waves (Figure 7). Both the duration of heat waves with high sWBGTX as well as the exposed population increased remarkably.

The total population exposed to extreme heat stress (Figure 10c,d) revealed a temporal evolution similar to the one for harsh conditions (Figure 9c,d), but lower magnitudes were observed compared to the 3 days threshold, especially during 1915-1955. Since 1998 more than 100 million people were exposed to extreme conditions. The percentile of the population affected by extreme heat stress, remained below 10 % for MED and CEU until 1990, after which this value was exceeded frequently. Additionally, a period of extreme heat stress exposure was identified for EEU after 1990 and even NEU experienced more than 5% population exposure in 2010.

The strongest significant trend was calculated for MED with an increase of 15% of total population per century. Increases of 7% per century for CEU and 11% per 100 years for EEU were found. On the other hand, the trend for NEU did not exceed 1% per century. Trends for population independent data (Figure A2), revealed significant trends similar to those of exposed population discussed above.

4. Discussion

The ERA-20C reanalysis data has good quality over Europe during the whole time series (1900-2010), as the density of observations is high throughout the 20th-century [Poli et al., 2016]. However, biases in 2 m temperature and dew point temperature may appear because temperature and humidity observations were not used for the data assimilation. Poli et al. [2016] identified a slight cold bias of 0.5-1K in temperature throughout the 20th-century with respect to nigh-time air temperatures observed by ships. Also, TX values may be underestimated by a few degrees Celsius in this thesis as we use data from 00:00, 06:00, 12:00 and 18:00 GMT which may not capture the daily maximum temperature over central Europe. Thus, less heat wave days are identified in this thesis compared to a study using a higher temporal resolution of ERA-20C, for areas where the threshold of TX ≥ 28°C is the restricting condition.

The trends in mean TX during the time series indicate significant warming in wide European areas (Figure 3). This is in line with the overall warming demonstrated by Moberg et al. [2006]. An increase of TX by more than 1°C is observed over Northern Russia, the Iberian Peninsula and Northern Italy. Similar warming over the Iberian Peninsula and Northern Italy was observed by Moberg et al. [2006] and Lorenz et al. [2019]. Further comparisons with observational and reanalysis datasets are necessary to quantify the relevance of the increases identified in this thesis.

The 98th percentiles increased more than the averages of TX and sWBGTX, indicating an increase in variability of the distribution in the upper 50 %, which is in line with the increase in variability observed by Lorenz et al. [2019]. In addition, Della-Marta et al. [2007] suggested an increase in daily summer maximum temperature of $1.27 \pm 0.32°C$ per century and increase in the variance of $5 \pm 2\%$ per century over the CEU region, which is slightly less than the TX98 over Western CEU identified in this thesis. A much greater trend is identified in Northern Russia, across the Balkans and Northern Italy exceeding 2°C. An increase across northern Italy of 1°C per 130 years was identified by Dole et al. [2011] for the period 1880-2009, but it exceeded 1°C towards West Germany, which is not in line with our results. The strong increases in TX and TX98 over Northern Russia might be explained by the intensified warming of the Arctic [Walsh, 2014].

The spatial extent of the 2010 Russia heat wave is similar to the extent identified by Russo et al. [2015] and the spatial pattern of the temperature anomalies found by Barriopedro et al. [2011] and Dole et al. [2011]. The DWD heat wave definition (Section 2.2.1) includes a fixed threshold, which is most certainly the reason for the lack of heat wave appearance in Northern Europe, that is observed for the 1972 heat wave as well. The 2003 heat

wave days distribution (Figure 5d-f) is similar to the analysis of Russo et al. [2015] but with differences over Northern Italy, whereas the spatial sWBGTX pattern shows more alignment with their analysis (see their Fig.2). Furthermore, TX spatial patterns are similar to the strong outgoing longwave radiation over northern Italy identified by Black et al. [2004]. The 2003 heat wave spatial extent is similar to the 3rd mode of Lau and Nath [2014] daily maximum temperature rotated empirical orthogonal function analysis. The heat waves from 1972 and 2010 are similar to their first mode, which indicates that their spatial distribution is typical for heat waves.

The heat wave definition used in this thesis is suitable to identify heat waves from the ERA-20C dataset over CEU, EEU and MED well. Further, the example heat waves are identified similar to the literature, as stated above. In addition to that, the heat wave definition was designed by the DWD for usage in Central Europe. In this thesis, fewer heat waves are identified over the UK and Scandinavia compared to McCarthy et al. [2019] and Russo et al. [2015], because they used a heat wave definition without a fixed threshold, thus indicating unusually warm conditions rather than both absolutely warm *and* unusually warm conditions.

The ERA-20C dataset showed a large increase in heat wave days per year from 1900-1930 to 1980-2010 over Europe, which agrees with the larger increases in TX98 compared to TX. A doubling of heat wave days per year (HWD/yr) is found over most of European with trends up to 4 HWD/yr/century over the Balkans, northern Italy and southern Turkey. An increase of more than 2 HWD/yr/century is identified across the Iberian Peninsula. An increase of 3 days for the maximum duration of heat waves (definition see Table A1) was observed in Northern Italy and the Iberian Peninsula, regarding the period of 1880-2005 by Della-Marta et al. [2007], which might be a factor that led to an increase in HWD/yr, found in this thesis. On the other hand, the occurrence of heat waves might have increased as well. To understand how both mechanisms affected the increase of HWD/yr, further analyses are required. Moreover, Lorenz et al. [2019] observed the largest increase in heat stress over the Iberian Peninsula, but they did not identify an increase in heat stress with a strong magnitude over the Balkans, thus partly resembling our results.

The sWBGTX exceeds the *alert* level [Sawka et al., 2003] of 26.7 during the period 1980-2010 in wide European areas, which was not the case during 1900-1930 (Figure 6). The later period, 1980-2010, also shows sWBGT above the *caution* level > 29.4 over northern France and along the coast of Italy and Cyprus. Strong significant trends in sWBGTX are observed in northern France and the Baltics.

Because the 95th percentile of the sWBGTX distribution during heat waves increases from 1900-1930 to 1980-2010 in Europe, the upper 5% exceed potential dangerous levels of 31.1 more frequently during the latter period. This most certainly causes serious health problems for the majority of the population.

The trends in HWD/yr can be certainly explained by the increase in TX98 (Figure 4). The strong TX98 increase in northern Russia is not visible for HWD/yr, because the threshold of 28°C still is not passed there. The increase in sWBGTX can partially be explained by TX increases because sWBGTX is linear dependent on TX (Equation (2)). The used reference period from 1961-1990 increases the chance to pass the criteria of the DWD definition.

Due to these trends, an increase in the exposed population was identified over Europe. Not the whole population will be exposed to heat stress during heat waves occurrence, due to regional and cultural adaptations (e.g. working indoors, resting during midday in the shadow). Physical conditions (e.g. age) play a crucial role in the impact of heat stress as well. Therefore only a fraction of the exposed population shown in Figure 9 and Figure 10 is actually affected by the heat stress. Therefore, differences in the demography and the state of health, fitness etc. between countries, amplify spatial heterogeneity of heat stress impact. Nevertheless, we can use it as a rough indicator of the impact on individual human health and society. The spatial pattern and the temporal evolution of the values help to compare between multiple regions and periods in a standardised way. Hence, the values demonstrated in this thesis are much higher than those observed by Feyen et al. [2020] and Watts et al. [2020], as both quantified the impact of heat stress on the population, taking health factors into account.

The regular (at least 5 years) exposure of European population, to harsh (Figure 9a,b) and extreme (Figure 10a,b) heat stress events increase from 1900-1930 until 1980-2010, especially in highly populated areas of MED and CEU. The increase in the exposed population can be explained with two approaches: first, the trends in HWD/yr (Figure 7f) can lead to more heat wave days fulfilling the conditions, even if the sWBGTX distribution does not change which is the case in Italy, the Balkans, southern Turkey and the Iberian Peninsula. On the other hand, trends in sWBGTX during heat waves (Figure 7d) can lead to a higher chance that sWBGTX exceeds the 98th percentile (1900-2010), even if no significant trend in HWD/yr can be seen which might explain the increase in wide parts of CEU.

The temporal evolution of population exposed to harsh and extreme heat stress during heat waves reveals pattern with alternating low (1900-1920), high (1920-1965), low (1965-

1985) and high (1985-2010) values. This pattern can be observed for the total European population and the percentile of the regional population (Figure 9c,d and Figure 10c,d). The percentile of the regional population exposed to extreme heat stress shows a strong increase after 1998 over CEU, MED and EEU. The values exceed 20% for MED and 10% for CEU and EEU after 1998.

An increase in the total population exposed to extreme heat stress is identified to be 15% per century for MED and 7% per century for CEU.

The temporal evolution of the population exposure to harsh and extreme heat stress is similar to the non-population-based long term analysis of heat waves occurrence by Della-Marta et al. [2007]. The phases of high and low population exposure identified in this thesis seem to follow the Atlantic Multidecadal Oscillation (AMO) phases analysed by Zampieri et al. [2017] and Trenberth et al.. This similarity would need to be further investigated to understand its relevance, as other atmosphere or ocean oscillations might influence the temporal pattern of the population exposed to severe heat stress.

The significant trends shown in this thesis must be interpreted with caution.
If for instance, only a *single* heat wave event occurred over a grid point, the trend of TX was derived *purely* from these few TX values. If it was significant concerning the rather short period (single heat wave), it was nevertheless projected to a change per century and marked as significant. Even though this trend is *not* based on climatological timescales, it might appear falsely as a significant climatological trend in Figure 7.

Areas which experience only a few heat waves during short periods (e.g. 5 years) are mainly affected by this issue. Further, this issue especially affects TX and sWBGTX trends, because these trends were based on daily values during heat waves. Trends in HWD/yr and exposed population were based on yearly sums which were 0 if no heat wave occurred which lead to continuous time series from 1900-2010.

The statistical analysis used in this thesis may not match all the approaches performed, and better statistical analysis are required to validate the relevance of the trends during heat waves shown in Figure 7. It may make sense to use a much larger data set, e.g. a grand ensemble 100 model simulations, to validate the trends.

5. Conclusions and Outlook

The DWD definition for heat waves used in this study is capable of identifying heat waves and their properties over wide parts of Europe, using the ERA-20C 2m temperature and dew point temperature. Nevertheless, fewer heat waves are identified in northern Europe compared to the literature [McCarthy et al., 2019; Russo et al., 2015], due to the use of a fixed threshold of 28°C.

In this thesis doubling in HWD/yr and strong increases in extreme TX and sWBGTX are observed over wide parts of Europe, indicating climatological increases of heat stress and heat wave occurrence during the 20th century. Thus, the increases in heat stress and heat wave occurrence identified by Lorenz et al. [2019] and Russo et al. [2015] can be considered as part of a climatological change over Europe which appeared throughout the whole 20th-century. This climatological trend, will be persistent in the future as suggested by Fischer and Schär [2010], Russo et al. [2015] and Feyen et al. [2020]. Further, shifts in sWBGTX distributions are the clearly visible over European Regions (CEU,EEU,MED and whole Europe) during heat waves, resulting in potentially dangerous heat stress already becoming more common throughout the 20th century.

We find a strong increase in the population exposed to severe heat stress throughout the 20th-century, which is similar to the global analysis by Watts et al. [2020] (supporting material) after 1980. Using the long time-series provided by ERA-20C allowed us to identify a multidecadal pattern of the European population exposed to severe heat stress. Its latest high phase is in line with the heat stress increase observed by Lorenz et al. [2019]. Future predictions of European population exposed to severe heat stress were found by Feyen et al. [2020] may be affected by this multidecadel temporal evolution which seems to follow the Atlantic Multidecadal Oscillation (AMO) phases analysed by Zampieri et al. [2017] and Trenberth et al..

The connection between heat waves over Europe and the AMO is of interest for follow-on studies, because this could modulate the impact of climate change on the occurrence of heat waves, on decadal scales.

A comparison with observational data sets including temperature and humidity would help to quantify the relevance of the results of this thesis, regarding the long time series of the ERA-20C dataset. The usage of large model ensembles, e.g. the MPI-ESM grand ensemble with 100 realisations of the period 1850-2005 and future climates, would allow to validate the results of this thesis and study the effect of anthropogenic climate change on heat waves.

The regional and cultural adaptations should be analysed because they have a significant impact on how humans are affected by severe heat stress in reality, although this would add several degrees of complexity to the population analysis. These adaptations might change in the future due to climate change. If for instance, Germany will expect similar heat wave statistics in the future climate, as the Mediterranean regions use to have today, the Siesta may become more important in Germany (which would be a benefit).

Results could be combined with environmental responses (to heat waves) to estimate how the decrease of basic health is related to heat stress and how its impact is amplified by environmental development, such as a combination with crop failure. Against this background, it is even more important to link the latest scientific knowledge from climatology and meteorology with the latest scientific knowledge from other disciplines

6. References

Alexander, L. V. . Global observed long-term changes in temperature and precipitation extremes: A review of progress and limitations in IPCC assessments and beyond. *Weather Clim. Extrem.*, 11:4–16, 2016. ISSN 22120947. doi:10.1016/j.wace.2015.10.007.

Australian Bureau of Meteorology. Thermal Comfort observationsn (last access 14 Dec. 2020), 2020. URL http://www.bom.gov.au/info/thermal_stress/#approximation.

Barriopedro, D. , Fischer, E. M. , Luterbacher, J. , et al. The hot summer of 2010: Redrawing the temperature record map of Europe. *Science (80-.).*, 332(6026):220–224, 2011. ISSN 00368075. doi:10.1126/science.1201224.

Black, E. , Blackburn, M. , Harrison, G. , et al. Factors contributing to the summer 2003 European heatwave. *Weather*, 59(8):217–223, 2004. ISSN 14778696. doi:10.1256/wea.74.04.

Buzan, J. R. , Oleson, K. , and Huber, M. . Implementation and comparison of a suite of heat stress metrics within the Community Land Model version 4.5. *Geosci. Model Dev.*, 8(2):151–170, 2015. ISSN 19919603. doi:10.5194/gmd-8-151-2015.

Center for International Earth Science Information Network - CIESIN - ColumbiaUniversity. Gridded Population of the World, Version 4 (GPWv4): Population Density, Revision 10, 2017. URL https://doi.org/10.7927/H4DZ068D.

Della-Marta, P. M. , Haylock, M. R. , Luterbacher, J. , and Wanner, H. . Doubled length of western European summer heat waves since 1880. *J. Geophys. Res. Atmos.*, 112(15):1–11, 2007. ISSN 01480227. doi:10.1029/2007JD008510.

Deutscher Wetter Dienst. Wetterlexikon - Hitzewelle (last access 14 Dec. 2020), 2020. URL https://www.dwd.de/DE/leistungen/rcccm/int/rcccm_int_hwkltr.html.

Dole, R. , Hoerling, M. , Perlwitz, J. , et al. Was there a basis for anticipating the 2010 Russian heat wave? *Geophys. Res. Lett.*, 38(6):1–5, 2011. ISSN 00948276. doi:10.1029/2010GL046582.

Dosio, A. , Mentaschi, L. , Fischer, E. M. , and Wyser, K. . Extreme heat waves under 1.5 °c and 2 °c global warming. *Environ. Res. Lett.*, 13(5), 2018. ISSN 17489326. doi:10.1088/1748-9326/aab827.

Feyen, L. , Russo, S. , Naumann, G. , et al. Global warming and human impacts of heat and cold extremes in the EU. 2020. ISSN 1831-9424. doi:10.2760/47878.

Fischer, E. M. and Schär, C. . Consistent geographical patterns of changes in high-

impact European heatwaves. *Nat. Geosci.*, 3(6):398–403, 2010. ISSN 17520894. doi:10.1038/ngeo866.

Iturbide, M. , Gutiérrez, J. M. , Alves, L. M. , et al. An update of IPCC climate reference regions for subcontinental analysis of climate model data: Definition and aggregated datasets. *Earth Syst. Sci. Data Discuss.*, (January):1–16, 2020. ISSN 1866-3508. doi:10.5194/essd-2019-258.

Lau, N. C. and Nath, M. J. . Model simulation and projection of European heat waves in present-day and future climates. *J. Clim.*, 27(10):3713–3730, 2014. ISSN 08948755. doi:10.1175/JCLI-D-13-00284.1.

Lorenz, R. , Stalhandske, Z. , and Fischer, E. M. . Detection of a Climate Change Signal in Extreme Heat, Heat Stress, and Cold in Europe From Observations. *Geophys. Res. Lett.*, 46(14):8363–8374, 2019. ISSN 19448007. doi:10.1029/2019GL082062.

Masson-Delmotte, V. , Zhai, P. , Pörtner, H.-O. P. , et al. Global Warming of 1.5°C. An IPCC Special Report on the impacts of global warming of 1.5°C above pre-industrial levels and related global greenhouse gas emission pathways, in the context of strengthening the global response to the threat of climate change,. *Ipcc - Sr15*, 2(October): 17–20, 2018. URL www.ipcc.ch/sr15/.

McCarthy, M. , Armstrong, L. , and Armstrong, N. . A new heatwave definition for the UK. *Weather*, 74(11):382–387, 2019. ISSN 14778696. doi:10.1002/wea.3629.

Moberg, A. , Jones, P. D. , Lister, D. , et al. Indices for daily temperature and precipitation extremes in Europe analyzed for the period 1901-2000. *J. Geophys. Res. Atmos.*, 111 (22), 2006. ISSN 01480227. doi:10.1029/2006JD007103.

Poli, P. , Hersbach, H. , Dee, D. P. , et al. ERA-20C: An atmospheric reanalysis of the twentieth century. *J. Clim.*, 29(11):4083–4097, 2016. ISSN 08948755. doi:10.1175/JCLI-D-15-0556.1.

Robinson, P. J. . On the definition of a heat wave. *J. Appl. Meteorol.*, 40(4):762–775, 2001. ISSN 08948763. doi:10.1175/1520-0450(2001)040<0762:OTDOAH>2.0.CO;2.

Russo, S. , Dosio, A. , Graversen, R. G. , et al. Magnitude of extreme heat waves in present climate and their projection in a warming world. *J. Geophys. Res. Atmos.*, 119 (22):12,500–12,512, 2014. ISSN 21698996. doi:10.1002/2014JD022098.

Russo, S. , Sillmann, J. , and Fischer, E. M. . Top ten European heatwaves since 1950 and their occurrence in the coming decades. *Environ. Res. Lett.*, 10(12), 2015. ISSN 17489326. doi:10.1088/1748-9326/10/12/124003.

Sawka, M. , Wenger, C. , Montain, S. , et al. Heat Stress Control and Heat Casualty Management. page 73, 2003. URL https://www.researchgate.net/publication/235183977_Heat_Stress_Control_and_Heat_Casualty_Management.

Sherwood, S. C. and Huber, M. . An adaptability limit to climate change due to heat stress. *Proc. Natl. Acad. Sci. U. S. A.*, 107(21):9552–9555, 2010. ISSN 00278424. doi:10.1073/pnas.0913352107.

Smith, T. T. , Zaitchik, B. F. , and Gohlke, J. M. . Heat waves in the United States: definitions, patterns and trends. *Clim. Change*, 118(3-4):811–825, jun 2013. ISSN 0165-0009. doi:10.1007/s10584-012-0659-2. URL http://link.springer.com/10.1007/s10584-012-0659-2.

Sonntag, D. . Important new values of the physical constants of 1986, vapour pressure formulations based on the ITS-90, and psychrometer formulae. *Vap. Press. Formul. based ITS-90 Psychrom. Formulae*, (Zeitschrift für Meteorologie. 1990, Vol 40, Num 5): 340 – 344, 1990. URL https://www.ptb.de/cms/en/ptb/fachabteilungen/abt3/fb-34/ag-341/publications.html.

Swedish Meteorological and Hydrological Institute. Värmeböljor i Sverige (last access 10 Dec. 2020). FAKTABLAD(49), 2011. URL https://www.smhi.se/polopoly_fs/1.16889!/webbFaktablad_49.pdf.

Trenberth, Kevin, Zhang, et al. The Climate Data Guide: Atlantic Multi-decadal Oscillation (AMO) (last access 14 Dec. 2020). URL https://climatedataguide.ucar.edu/climate-data/atlantic-multi-decadal-oscillation-amo.

Walsh, J. E. . Intensified warming of the Arctic: Causes and impacts on middle latitudes. *Glob. Planet. Change*, 117:52–63, 2014. ISSN 09218181. doi:10.1016/j.gloplacha.2014.03.003.

Watts, N. , Amann, M. , Arnell, N. , et al. The 2020 report of The Lancet Countdown on health and climate change: responding to converging crises. *Lancet*, 0(0), dec 2020. ISSN 01406736. doi:10.1016/S0140-6736(20)32290-X. URL https://linkinghub.elsevier.com/retrieve/pii/S014067362032290X.

World Health Organization. Heatwaves (last access 14 Dec. 2020). 2020. URL https://www.who.int/health-topics/heatwaves#tab=tab_1.

World Meteorological Organization. Guidelines on the Defintion and Monitoring of Extreme Weather and Climate Events (last access 14 Dec. 2020). *Task Team Defin.*

Extrem. Weather Clim. Events, (December 2015):62, 2018. URL https://www.wmo.int/pages/prog/wcp/ccl/opace/opace2/TT-DEWCE-2-2.php.

Zampieri, M. , Toreti, A. , Schindler, A. , et al. Atlantic multi-decadal oscillation influence on weather regimes over Europe and the Mediterranean in spring and summer. *Glob. Planet. Change*, 151:92–100, 2017. ISSN 09218181. doi:10.1016/j.gloplacha.2016.08.014.

Appendix

List of abbreviations

T	°C	Temperature
TX	°C	Daily maximum temperature
TX98	°C	98th percentile of the daily maximum temperature
WBT	°C	Wet Bulb Temperature
WBGT	°C	Wet Bulb Globe Temperature
sWBGT	unitless	Simple Wet Bulb Globe Temperature
sWBGTX	unitless	Daily maximum simple Wet Bulb Globe Temperature
sWBGTX98	unitless	98th percentile of the daily maximum simple Wet Bulb Globe Temperature
HWD	days	Heat wave days
HWD/yr	days per year	Heat wave days per year
HI	°C (USA: °F)	Heat Index

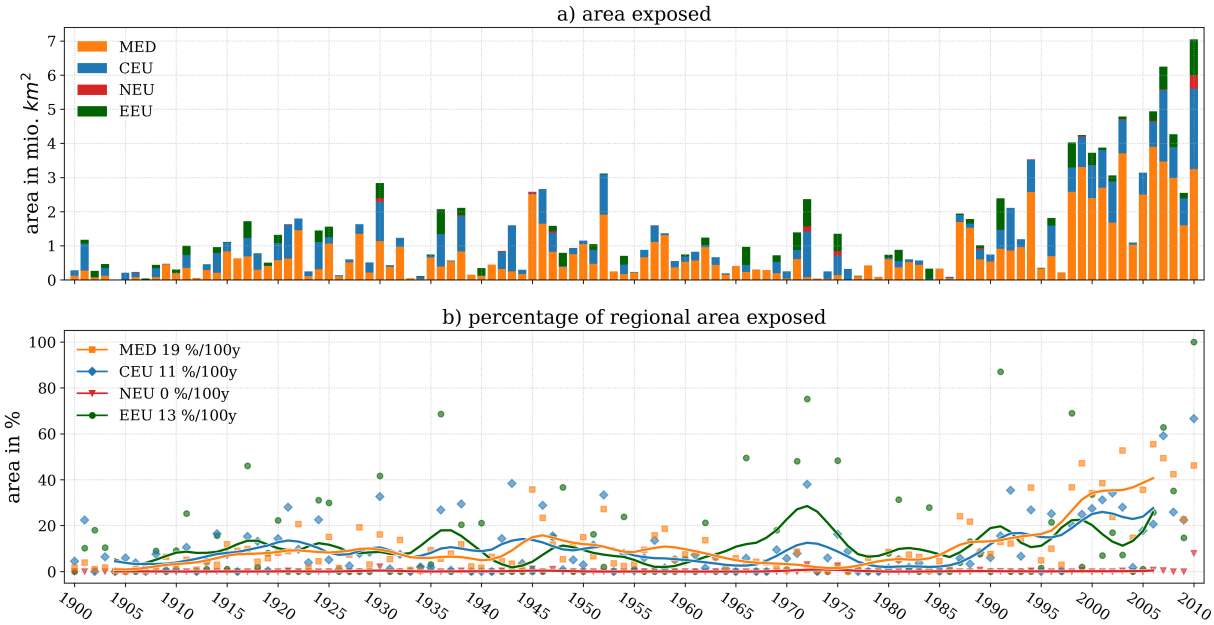

Figure A1: Area exposed to at least 3 heat wave days per year with sWBGTX value being part of the upper 2% (1900-2010). a) Total area b) percentage of area with solid lines being Gaussian filter of $\sigma = 2$years. Significant trends for each region in the legend.

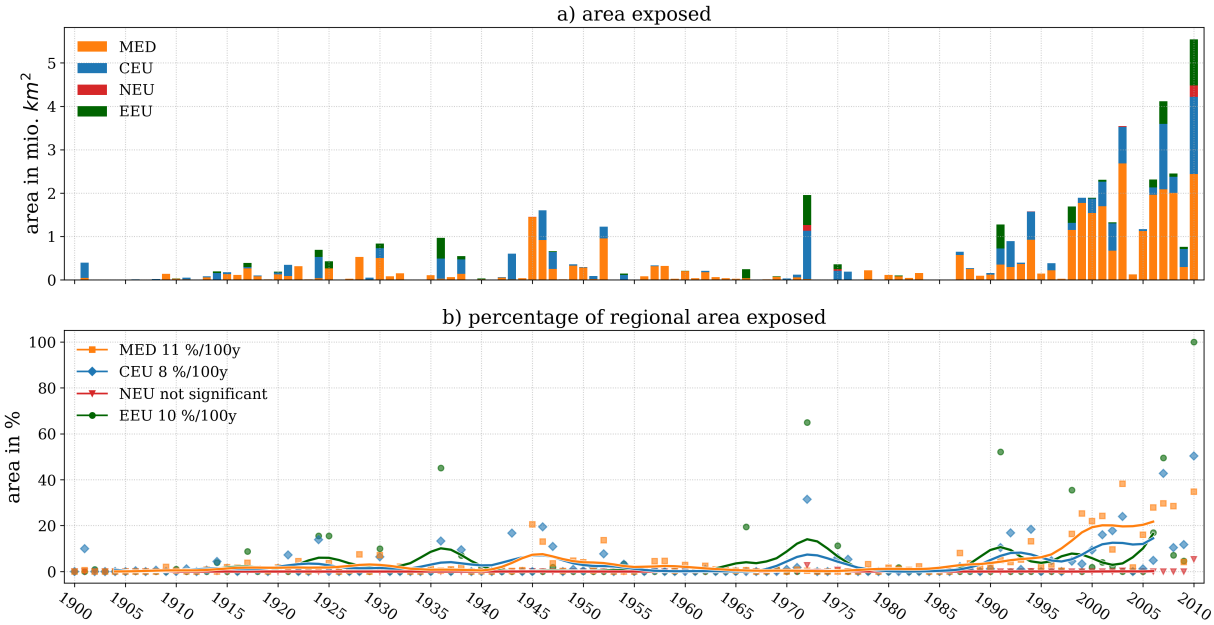

Figure A2: Area exposed to at least 6 heat wave days per year with sWBGTX value being part of the upper 2% (1900-2010). a) Total area b) percentage of area with solid lines being Gaussian filter of $\sigma = 2$years. Significant trends for each region in the legend.

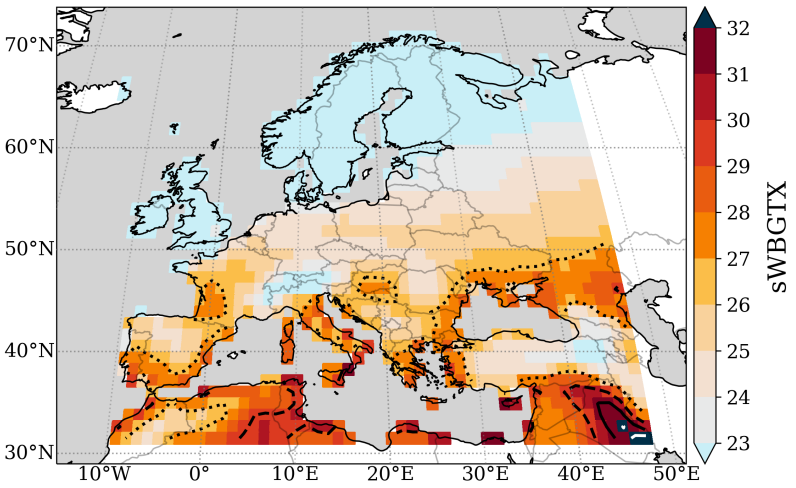

Figure A3: sWBGTX 98th percentile (1900-2010) used as sWBGTX percentile threshold in Section 3.4. Contour lines as sWBGT threat levels: alert (dotted black), caution (dashed black), potential danger (solid black), dangerous (solid white) (see Table 1).

Table A1: Comparison of heat wave definitions

References	Duration	Definition
Deutscher Wetter Dienst [2020]	$\geq$ 3 days	TX $\geq$ 28°C TX $\in$ 98th percentile of $\bigcup_{y=1961}^{1990} \bigcup_{i=d-15}^{d+15} TX_{y,i}$ Reference period: 1961-1990
Robinson [2001]	$\geq$ 2 days	HI night-time low $\geq$ 26.7°C HI day-time $\geq$ 40.6°C HI $\in$ 98th percentile of HI Reference period: 1952-2015
Feyen et al. [2020]; Russo et al. [2014, 2015]	$\geq$ 3 days	TX $\in$ 90th percentile of $\bigcup_{y=1981}^{2010} \bigcup_{i=d-15}^{d+15} TX_{y,i}$ Reference period: 1981-2010
Della-Marta et al. [2007]	= maximum number of consecutive days found in June-August	TX $\in$ 95th percentile of $\bigcup_{y=1909}^{1990} \bigcup_{i=d-7}^{d+7} TX_{y,i}$ TX during June-August Reference period: 1909-1990
McCarthy et al. [2019] (designed for the UK)	$\geq$ 3 days	TX $\in$ 90th percentile of $\bigcup_{y=1981}^{2010} \bigcup_{i=d-7}^{d+7} TX_{y,i}$ Reference period: 1981-2010
Swedish Meteorological and Hydrological Institute [2011] (designed for Sweden)	$\geq$ 5 days	TX $\geq$ 25°C

Eidesstattliche Erklärung

Hiermit erkläre ich, dass ich die vorliegende Arbeit selbständig und ohne fremde Hilfe angefertigt und keine anderen als die angegebenen Quellen und Hilfsmittel verwendet habe. Die eingereichte schriftliche Fassung der Arbeit entspricht der auf dem elektronischen Speichermedium. Weiterhin versichere ich, dass diese Arbeit noch nicht als Abschlussarbeit an anderer Stelle vorgelegen hat.

Datum: _____ Unterschrift: _____